Industrial Robot Based 3D printer

João Domingues Alves Cantante Pires

joao.d.pires@tecnico.ulisboa.pt

Instituto Superior Técnico, Universidade de Lisboa, Lisboa, Portugal
November 2021

***Abstract*—This work aims to study the feasibility of using an ABB IRB 140, an industrial robotic arm, as a positioner for FDM 3D printing. In this project a CNC was also implemented just as a proof of concept. To accomplish this project, Siemens NX was used, where all the operations were developed, simulated and post-processed in RAPID code. The generated code was interpreted by Robotstudio®, a program developed by the robot's manufacturer, which allows for error detection and collision prevention. To test the positioner's characteristics, a test specimen was developed, printed at various speeds. To obtain a measurable understanding of the results obtained on the test specimens, the acceleration of these printing routines was measured through an accelerometer placed on the robot's end-effector. These accelerations were compared with the defects observed on the test specimens, and with studies previously developed on this robot, to obtain clear conclusions.**

Key Words—Industrial Robotic Manipulator, FDM 3d printing, Robotic 3d printer, Robotic CNC.

I. Introduction

This paper seeks to characterize, through a test specimen specially developed for the purpose, the capabilities of an ABB IRB 140 as a positioner for 3D printing operations, and prove the validity of the hybrid additive-subtractive robotic manufacturing concept

A. Developed Work

To characterize the robot, this work:

- Starts by simulating virtually and dynamically the experimental setup of this project.
- Simulates and post-processes printing operations of the test specimen.
- Through FDM 3D printing, obtains physical models of the specimen.
- Compares the results obtained by the test parts with acceleration measurements at the end-effector of the robot.
- Draws conclusions, through the analysis of a work previously developed on this manipulator, confirming those results with manuals provided by the manufacturer.

II. Setup

A. Materials

To simulate these operations Siemens NX was used, allowing a high flexibility of tools, machines, operations, and post-processing capabilities that made this test possible, and that will make possible future more complex projects related to this subject.

The extruder used was a direct drive, non-geared, single driven unit, allowing the best compromise between price, and extrusion capacity. Controlled by an Arduino MEGA, a RAMPS 1.4 shield, running and open source 3d printing firmware *marlin*.

The printing material utilized was Poly Lactic Acid (PLA). Since no special mechanical properties were required, this material was chosen, because it known for its ease of printing, requiring no special storing conditions, and because it is commercially available at a low price.

As a printing surface, a glass bed was used, since glass is a fragile yet hard material, having a low thermal conductivity.

These properties ensure that there is no significant deformation along its surface, allowing for a leveled surface on all the printing area through the leveling of its four corners. Its hardness allows the printed parts to stay clear of defects on the first layer, and guarantee excellent bed adhesion and part removal, since its surface it will not scratch, even when cleaned it with metallic scraper. Its low thermal conductivity will ensure a constant heat distribution through the bed's surface, preventing deformation problems.

As a positioner the industrial robot arm used is an IRB 140, developed by ABB Robotics. This anthropomorphic robot with 6 degrees of freedom, has a payload capacity of 6kg, with a maximum linear speed of 2500 mm/s, a minimum of 1mm/s and a minimum joint resolution of 0.01 (deg.).

B. PLA Extrusion Parameters

Through the analysis of some mechanical studies made to this material, printed in 3D with layer heights ranging from 0.1 to 0.3 mm, we obtain that:

"Apparently, the tensile failure strength of this FDM 3D printing PLA material with the same printing angles becomes bigger as its layer thickness decreases from 0.3 mm to 0.1 mm.". [1]

"In this study, two printing parameters, layer height and plate temperature, were explored to understand their effects on the Izodimpact strength of printed PLA. Observations on the crosssection of printed PLA showed that a printing setting of 0.2 mm layer height and 60ºC plate temperature produced smaller voids inside the parts attributed to an improved degree of diffusion." [2]
"From the above results, it can be clearly observed that specimens prepared with 0.2 mm layer thickness, 0º orientation and a printing speed of 38 mm/s exhibited a maximum flexural strength properties […]. "[3]
"Comparing to other authors, we conclude the same as in (Wittbrodbt et al, 2015; Tymrak et al. 2014; Lanzotti et al. 2015b) regarding the tensile testing. The best values of σuts, σY and E correspond to experiment #21 with an infill of 60%, an extrusion temperature of 220ºc, a raster angle of 0º/90º and a layer thickness of 0.1 mm"[1]
"Ultimate Tensile Strength, the Yield Tensile Strength and Modulus of Elasticity show its best values for an Extrusion Temperature of 220ºC, a Raster Angle of 0º/90º and a Layer Thickness of 0.1 mm. On the other hand, the Elongation at Break and the Toughness show its best results for an Extrusion Temperature of 200ºC, a Raster Angle of -45º/+45º and a Layer Thickness of 0.2 mm."[1]

And thus the following table was obtained, with the following recommended extrusion parameters, by the previous authors:

Tabela 1- Printing parameters

Nozzle Temperature	Layer height	Layer Width
210 ºC	0.2 mm	0.5mm

C. Extrusion Planning

Before extruding, it is important to make sure that the extruder extrudes exactly the amount of filament we want. When increasing the extrusion speed, the motor no longer has the torque to force filament through the nozzle.
Please note that with a higher temperature in the nozzle it is possible to achieve higher extrusion speeds.

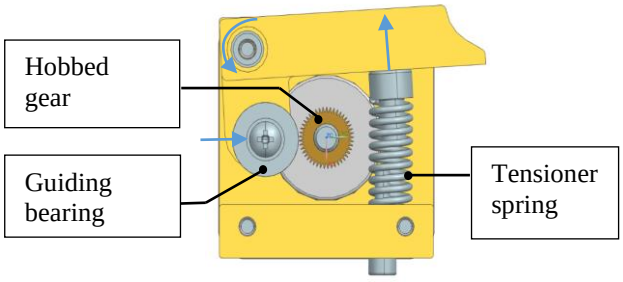

Figure 1- Extruder tensioner guide

This is especially important in our extruder since there are no reduction gears between the stepper motor and the gear that pushes the filament into the nozzle. Therefore, extra care had to be applied when adjusting the tension between the hobbed gear and the extruder guiding bearing to maximize this speed.
To start, we will tune the motor's steps in the extruder's firmware. At first, we calculate an approximate value that we would expect for the number of steps needed to extrude 1mm of filament:

Hobbed gear diameter- 10.95 mm (aprox.)
Motor Resolution – 200 steps/revolution
Driver resolution - 1/16 revolution/step

Unit resolution:

$$P = \pi * 10.95 = 34.38\ mm/rev \quad (1)$$

$$resol = 200 * 16 = 3200\ step/rev \quad (2)$$

$$\frac{3200}{34.38} = 93\ steps/mm \quad (3)$$

Now we will place our filament on a ruler, mark a position, and extrude 50 mm of filament, considering the approximate calculated value and measure that result.

Amount extruded – 47.9mm (aprox)

$$P = \pi * 10.95 = 34.38\ mm/rev \quad (4)$$

$$\frac{93 * 50}{47.9} = 97.08\ steps/mm \quad (5)$$

After updating this value on the *marlin* firmware, we verified that this value holds true for various speeds.
Now with the calibrated extruder, we will start incrementing the speed until the motor can't extrude the exact desired amount. This can happen due to slippage between the hobbed gear and the filament, or when the motor reaches its torque limit. The tensioner spring can be tuned to prevent slippage, at the compromise of torque limitation, for the extruder motor.
The maximum extrusion value was found to be 160mm/min (2.667 mm/s).

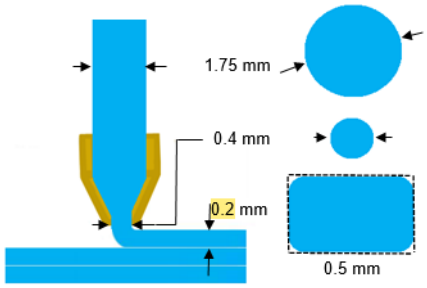

Figure 2-instant areas

According to the image above, we are going to calculate the extrusion speed, matching the feed rate on the robot. In Figure 2 we saw three moments in which the area of the part changes, the filament, with 1.75 mm diameter, the exit of the nozzle

(instant 0), with 0.4 mm diameter, at the exit of the nozzle (instant 1), and the deposited filament (instant 2), which we will approximate to a $0.5mmX0.2mm$ rectangle.
Applying an area conservation between the initial filament, and the deposited filament we have:

$$A_0 v_0 = A_2 v_2 \quad (6)$$

Having v_0 as the extrusion speed v_e and v_2 as the feed rate imposed by the robot's TCP speed v_r:

$$\frac{\pi * 1.75^2}{4} * v_e = 0.2 * 0.5 * v_r \quad (7)$$

$$v_e = \frac{0.2 * 0.5 * 4}{1.75^2 * \pi} * v_r \ (mm/s) \quad (8)$$

Using this equation, we can now calculate the extrusion speed having the robot's TCP speed.
Using this equation, we can also verify, that the maximum printing speed, limited by the extruder, is 64.14 mm/s.

III. Results

In this chapter, we will discuss the defects obtained, in accordance with the acceleration graphs obtained. Different speeds highlight different observed particularities in the quality of the prints, which will be more and less evident according to each speed.
It is always useful to stress that the goal of this work is to evaluate the ABB IRB 140 as a positioner for 3d printing, and not the qualities of the setup. This is why the focus of the work is around this thin square, a simple yet interesting piece for evaluating the quality of the positioner.
With the part designed, several tests were made, where we only varied the robot's feed rate, in accordance to its respective calculated extrusion speed, at 30, 40, 50, 60 and 70 mm/s of feed speed. With these was found that, on the parts, essentially two main defects occur, which unfold in their sub-problems.

A. Defects Observed

At predominantly lower speeds, the parts had problems regarding surface finish. Was found that the surface finish on the X and Y oriented surfaces have different characteristics. While the surfaces oriented in the Y axis suffer a phased waviness with a high wavelength, creating vertical stripes, the surfaces oriented in X have a much lower wavelength, with an offset, which causes diagonal stripes.

Figure 3- X surface and Y surface comparison

As speed is increased these ripples on the surface becomes less pronounced, caused by an increase in the wavelength and an apparent loss of amplitude of these waves.

Figure 4- X surface v30,v40,v50

At higher speeds we start to have problems in the corners, which start to appear very lightly at 40mm/s and become critical at 60mm/s, making quality parts impossible to print.
What happens in these parts is that there is a decay of material in the corners that occurs in the direction of the previous movement of the corner, that is, if the previous corner has been described in X, when the movement is switched to Y and a clear reverberation can be seen in the x-axis, as the new movement is described in along the y-axis.

Figure 5- v50 corner defect

Also related to this problem of corner quality, was observed that there is a clear difference in relation to this intensity of reverberance trough the four corners. From the picture below, we can see clear differences in the finish between corner 1, 2, 3 and 4 form the same part.

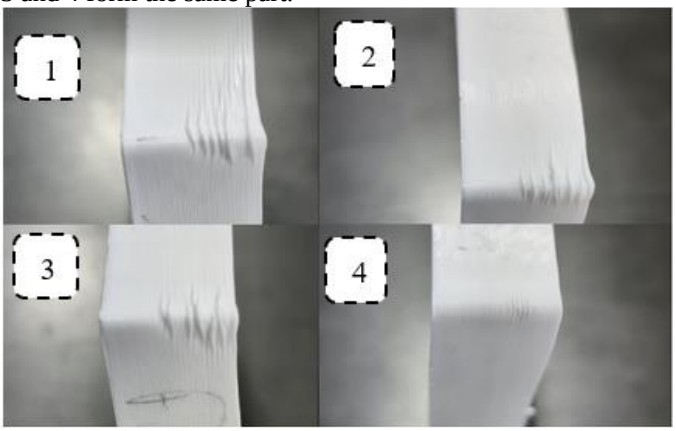

Figure 6- Corner Results V50

Also minding this corner problem, a layer thickening around the corners could be observed. Although this does not stem from the same problem as the previous paragraph, it does help to make it more noticeable.

It also is important to note that the calculated extrusion fulfils the calculated dimensioning, at the proposed speeds. It was expected that the filament assumes a slightly higher thickness, since the round section filament does not deposit with a purely rectangular section, but, a rectangular section, with rounded corners. As the layer height is imposed by the TCP motion, in order to maintain a constant extrusion flow rate, it is expected that the extrusion width will be slightly larger than projected.

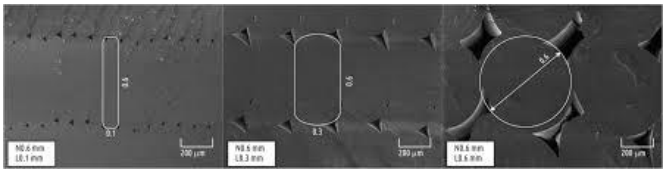

Figure 7- Microscopic Layer analysis (illustrative)

Given the problems with surface irregularity, it is not relevant to calculate this radius of deposited filament, as its width will vary on the surface. Here we just want to show that the extrusion design holds true.

Using a micrometer, it was possible to verify that the layer width, at the center of the edges, had a value close to the projected thus validating the design method for layer project.

B. Surface quality

1) Basic robot movement

Having now the simulation matching the measured graphs, and the Z offset corrected, we can have a proper critic analysis on some measured results.

For a total acceleration graph would be expected, high peaks at Max acceleration when the robot changes direction between the X and Y axis.

Since the movement in Z is an ascending spiral at constant rate, the expected acceleration on this axis is expected to be zero.

Therefore, this graph below would represent exactly what we can expect, in terms of total acceleration:

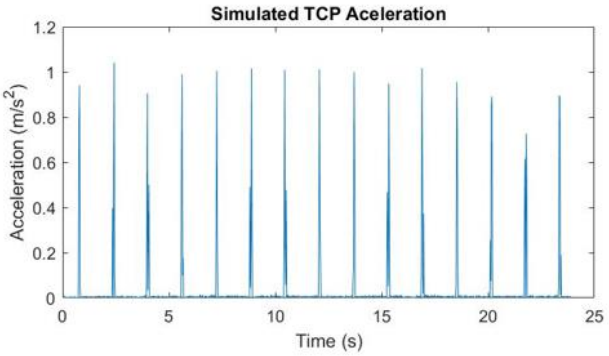

Figure 8-v30 Simulated TCP acceleration

The obtained graph for the total TCP measured acceleration shows a significant vibration where the acceleration is expected to be zero.

Moreover, the fact that in this vibration we can see a clear oscillation between the X and Y movements and this graph is not centered around zero, we get two strong indicators that this vibration is not only happening in one axis, and there is a probable vibration in more than one axis, creating a signal overlap, as we can confirm below.

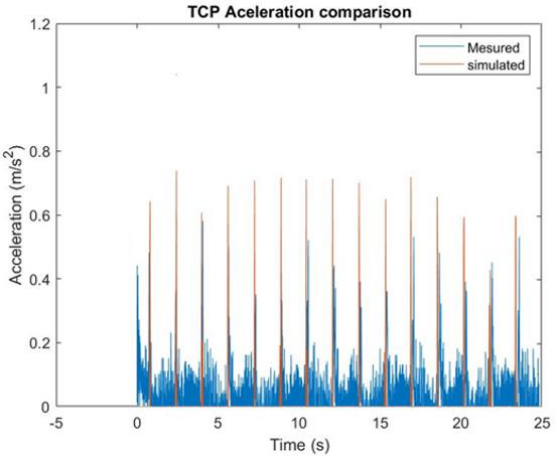

Figure 9-v30 TCP acceleration comparison

By separating the measured results into its XYZ acceleration components, we not only can see that there is in fact vibration, but also that this measured vibration also happens in the Z axis.

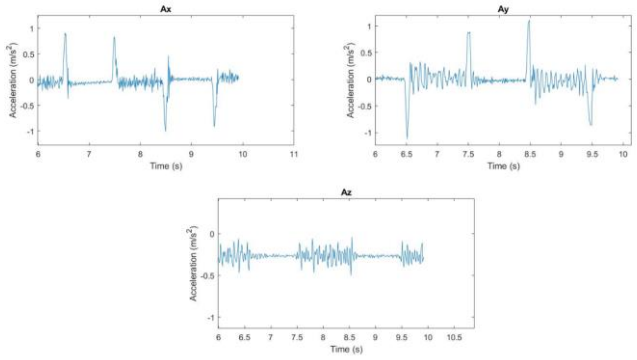

Figure 10- XYZ vibration

In the RAPID code generated by NX we get a first layer of 0.2mm, i.e the TCP is at 0.2mm of the defined position of zero, that, as we saw before actually correspond to a distance of (approx..) 0.3mm of the surface it is printing on.
Form the moment the bead crosses the initial deposition point, the TCP starts describing a spiralled ascending movement. For every two lines of code, the TCP advances 0.001mm in the positive direction of the Z axis, while for each line of code it advances 0.397mm either in the X axis or in the Y axis, depending on the edge it's describing.
So for every 0.794mm in the X or in the Y axis, the robot moves 0.001mm in the positive direction of Z.
And therefore, the speed in the XY plane is:

$$\frac{0.794}{0.794 + 0.001} * 100 = 99.874\% \qquad (9)$$

The total speed at wich the TCP is mooving.
So in the XY plane the TPC is moving at 29.962 mm/s ($99.87\% * 30\, mm/s$) and 0.0378 mm/s ($0.126\% * 30\, mm/s$) in the Z axis in the positive direction.
Considering the speed of 30mm/s (0.030m/s), two lines of code are executed every 0.0265s, according to:

$$\frac{0.794}{30 * 0.9987} = 0.0265\, s \qquad (10)$$

Thus, what we would expect for a Z acceleration plot would be a graph with acceleration peaks every $0.0265s$, at a constant period, during the hole print. Clearly, observing the graph below, this is not the case.

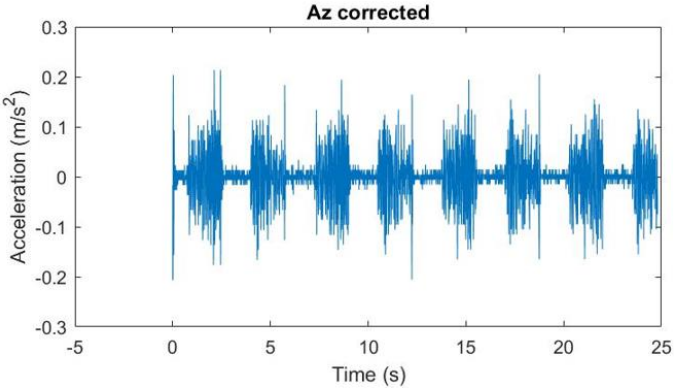

Figure 11- Az Correction

Apparently, it may look like the accelerometer may be misaligned, and take part of the of the x into z readings. Careful fine-tuning of the accelerometer was done to make sure this didn't happen.
Also in the XY plane, a vibration can be noted. To further illustrate this, a deep understanding of what we could expect graphically is expressed below.
For the XY graphs it would theoretically be expected that the graph would be as follows:
- It leaves the initial point where it had a peak of positive acceleration in Y, which would remain null until it ended in a negative peak, which would denote a deceleration that would switch the motion to the x-axis.
-Once it ended the movement in Y, it would begin the movement in X, again with a high negative peak in x. Note that, considering that the sensor is now moving in the negative direction, the accelerations are the reverse of we would expect. The acceleration would remain zero until the end of the edge, where it would have a high positive peak, which would demarcate the deceleration of the axis change.
-on the next two edges, the expected pattern of motion would be the reverse.
Again, this is clearly not the case.
When the robot describes an edge in Y, there is a constant vibration when the TCP moves in that direction.
Moreover, when describing an edge at x, we can verify the same thing, but with one particularity. When the motion is described in x, the same vibration is detected in the z-axis, that we can verify, by aligning the graphs, as seen below.

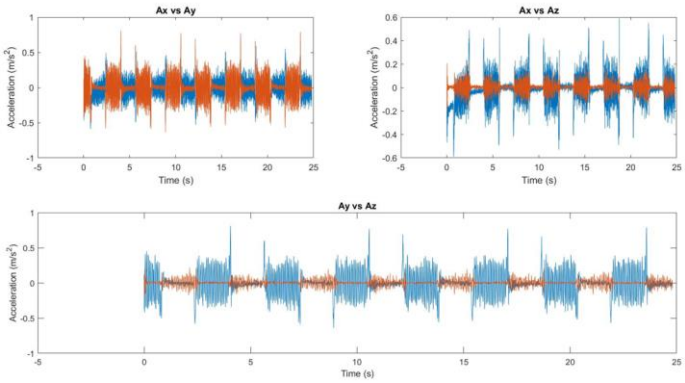

Figure 12- Ax Ay Ax comparison

Note that the TCP is able to travel at a maximum speed of 2500mm/s, where these vibrations are not felt. Considering that we print at a speed of 30 mm/s to 60 mm/s, we then work at speeds between 1.2% and 2.4% of the maximum speed of the robot, the of the robot.

By observation of the upper graph, it is clear to observe that when the robot moves in the Y direction, there is a vibration in the Y-axis, cantered around zero. When it moves in the X direction, no vibration are felt in Y.

To understand why there is an overlapping on the X and Z chart, we have to understand how the robot describes such a movement, and to help explain it we have the robot simulated joint speed graph below.

The y-motion is achieved by the movement of joint one and six. Since joint one in further away from the TCP, small movements on that joint will have a big affect on the x position of the TCP, while joint 6 just corrects the orientation of the TCP.

So joint 1 moves, vibrating, causing the movement to happen not at an instantaneous speed defined by the federate, but at an average speed, vibrating, causing the filament to have more and less thickness on the same surface, always with the same periodicity, creating this wavy effect.

Recovering the same analogy for X-movements, and analysing figure above we can see that in the y movements there are three joints involved, joint two, three and five.

Again the distance between the TCP and joint two and tree will be much more significant than to joint five.

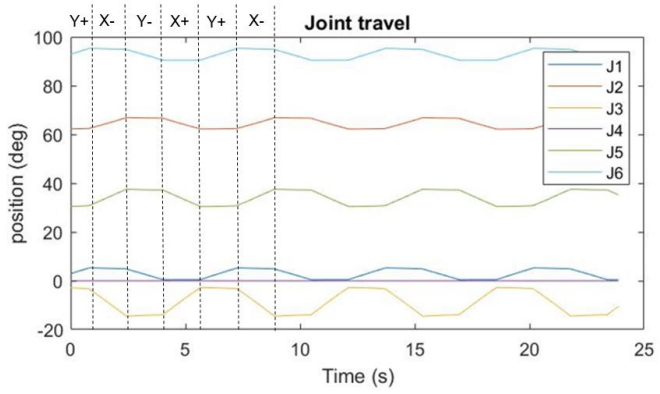

Figure 14- Simulated Joint travel

In an X+ movement what happens is that joint 3 opens while joint 2 closes, that is, they compensate each other.

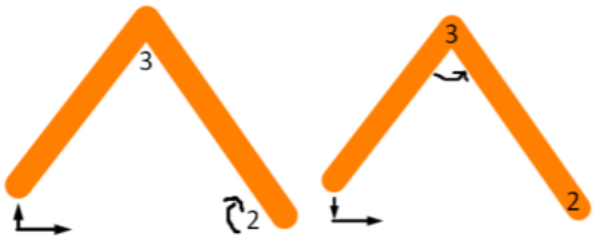

Figure 15-TCP X-movement

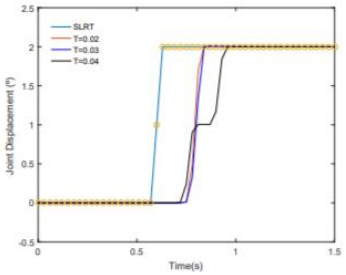

Figure 13- Adapted from [4]

In practical terms, what ends up happening is that joint 2 causes an acceleration and a movement in x+ and z- when it opens, which is then compensated by joint 3, which does exactly the opposite.

The hole motion along x happens this way, causing oscillations in X and Z, thus explaining why we can observe a vibration in the Z component of the accelerometer aligned with the x vibration.

From what I have explained above, we can easily understand why, also, the surface in the x-direction is also wavy but with a shorter period between waves. As this movement is given simultaneously by the compensation of two joints.

But why is a vibration felt, in the first place?

2) Vibration

To help explain this phenomenon, we will resort to a thesis developed on this same robot, by colleague Vasco Gama Caldas Sampaio in 2017. In this thesis, he studies in detail the communication between the robot, and the controller, where at the end of this chapter we will find that the answer to this problem is contemplated.

"To understand the delay introduced by the communication interface as well as the time required to run both programs, we ran only the algorithm that refers only to communication (see figures 3.13 and the algorithm in page 38). N sine wave were generated in SLRT, sent to the IRC5 and resent to SLRT. The time shift between the signals corresponds to the programming delay. A secondary goal of this test was to confirm that the SLRT fundamental sampling frequency is limited by baud rate.

[…]

In both cases, the minimum achieved sampling time for which no data is lost is st = 0.03s, which is close to the estimated. […] From this result we know that the update rate of the position variable (in RAPID) is 33Hz, therefore all the

following tests aim at giving the manipulator a dynamic behavior that complies with this rate."[4]
Through this test, it can be understood that the processing speed of the points is limited by a baud rate, i.e., if the sample time between points is less than the baud rate, and if the points are within the defined zonedata, the points are ignored, because the robot cannot respond to sample times less than 0.03s.
"By comparing both graphs, we can see that initial dead time is the same. This means that RAPID can resume execution, after a move function, fast enough to update position and call the next move function. We, therefore, conclude that it is useless to update two (or more) position variables before calling a move function. Thus, only one move function is required."[4]
The author, in order to confirm the above speculation, does a test, where he generates two positions at the same speed, but with sample times above and below the minimum communication frequency. What he verifies is that with a lower sample time, this intermediate position is ignored.
In the image above "[…]for \T = 0.04 its clear that, even with a zonedata defined, a trajectory could not be defined such that the first point behaved as a via point. Recall that when this happens, it is called a corner path failure. These have to be avoided, otherwise the resulting motion will be jerky and vibrations affect the force sensor."[4]
"Problems can occur if much logging to files is added in CAP and user event trap routines. The reason is that file writing takes long time and will delay the execution of the next instruction. That may cause corner path failure, stopping the movement of the robot for a short time, which may be fatal for the process (for example, arc welding)."[5]

"The Continuous Application Platform (CAP) consists of a number of RAPID instructions and data types that make development of continuous applications easier, faster, and more robust." [5]
"A CAP motion instruction (CapL or CapC) is similar to other motion instructions (for example, MoveL, TriggL)." [5]
This is exactly what happens in this routine, consisting of moveL instructions taken at a lower boudrate than supported.
To better support this theory, we went to the graphics where we verified this phenomenon and calculated the time difference between maximizers in the vibration zones and the amplitude measured from the x-coordinate of the maximiser to zero, obtaining the following results:

$$\Delta t_{MtoM}(v30) = 0.0681s$$

$$A_M(v30) = 0.2915\ m^2/s$$

$$\Delta t_{MtoM}(v40) = 0.0699s$$

$$A_M(v40) = 0.2020\ m^2/s$$

$$\Delta t_{MtoM}(v50) = 0.0645s$$

$$A_M(v50) = 0.1715\ m^2/s$$

As we speculated in the previous chapter, in fact as the velocity increases the vibration decreases, and the period in mm increases. Note here that the same time period between waves implies that at one speed a greater distance between dead zones is travelled.
Of even more interest, we can see that the peak-to-valley wavelength (half the value of the wavelength) is:

$$\Delta t_{M2m}(v30) = \frac{0.0681s}{2} = 0.3405s \quad (11)$$

$$\Delta t_{M2m}(v40) = \frac{0.0699s}{2} = 0.0350s \quad (12)$$

$$\Delta t_{M2m}(v50) = \frac{0.0645s}{2} = 0.0323s \quad (13)$$

Values very similar to the communication frequency between the controller and the robot.
Remembering that with a distance between points of 0.397m, we would have between points, a theoretical processing time of:

$$\Delta t_{p\ to\ p}(v30) = 0.0132s$$

$$\Delta t_{p\ to\ p}(v40) = 0.00993s$$

$$\Delta t_{p\ to\ p}(v30) = 0.00794s$$

We thus confirm that the ripple in this program is caused by the baud rate between the IRC5 and the ABB IRB 140.
In addition, the amplitude of the wave decreases, as we can see from the parts, and the acceleration graphs. This happens because the wavelength is longer, i.e., the robot reaches terminal velocity at a shorter distance, and therefore the deceleration that follows the acceleration is not as pronounced. In the limit, as abb argues, the motion should be described at the fewest possible points, for this effect to be felt only at the beginning and end of the motion, in this case a start and end point of the edges. Note that at 50mm/s these effects are already very difficult to observe in the part.

C. Corner quality

As it is verifiable, this problem of falling material in the corners, although not caused by layer thickening, is exalted by it. This thickening happens because the robot loses speed when approaching the corners, and this phenomenon is contemplated in the simulation, but the acceleration measured in the robot's TCP does not reach the simulated values, and what ends up happening is that there is a delay between the measured acceleration graphs and the simulated ones. This effect is noticeable at all speeds and gets worse as the speed increases. The lowest speed at which this effect starts to be noticeable is at 40mm/s, which in this case, induces at the end a total delay of:

$$\Delta t_{delay}(v40) = 249s - 247{,}5s = 1{,}5s \quad (14)$$

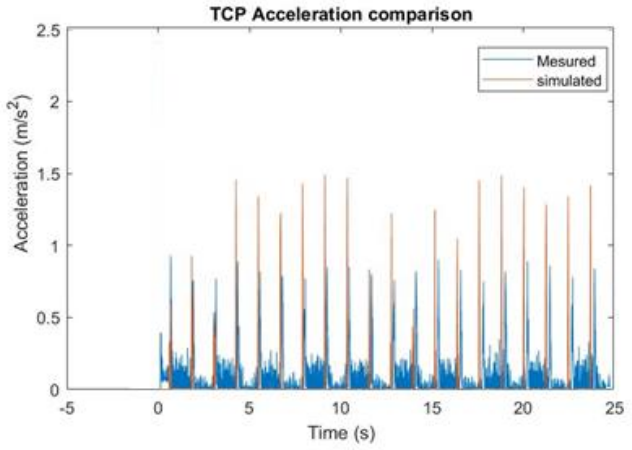

Figure 16-graph delay at 40mm/s

To ensure that the speed of the TCP did not vary considerably, affecting the thickness variation in the corners in such a way as to have a significant impact on the quality of the printed parts, the TCP zone was set at Z20.

In fact the effects of thickness variation, given the reduction of speed at the corners, can still be felt, and potentiate the harmful effects of resonance, z20 managed to be the best compromise between an approximately constant speed, and considerable resonance effects.

At the speed of 50mm/s is it verifiable that the simulated accelerations vary a lot according to the direction of the movement. Analyzing the graph above, a pattern is identifiable, which in fact is expected. As one can observe the total acceleration in the passage in corners 1 and 3 is higher than the accelerations in corners 2 and 4.

This happens because the stiffness of the robot is different in X and in Y.

This type of test is commonly known as the resonance test, in this case, the square was chosen as the test, and oriented with the edges in X and Y just to be able to test the effect of resonance in the transition between XY and YX.

Note that if the square was oriented diagonally, the resonance effects could not be measured, as the resonance in relation to the x and y axes would be distributed at the same 45°.

In simulation, at any speed the software assumes the robot as a rigid structure. Typically, industrial robotic arms have high rigidity, when compared to other types of robotic arms (medical, collaborative, etc), still the inertia of the robotic arms and its payload makes the joint motors of the robot no longer able to behave as rigid.

It is known that the robot behaves as a second order system, spring, mass, damper. Theoretically, the assembly should behave like a critically damped system, but curiously, this is not what we verified, because there is here a clear indicator of position overshoot, mainly in the YX corners.

In this movement we are interested in noticing the difference between the stiffness in X and in Y. Note that it will be different, in both directions, since, the moment produced by a force applied in the TCP in Y, to joint 1, will be much greater than the moment felt in joints 2 and 3 caused by the same force applied at the same point, in X, given the distances from the point of application to the joint in question. To summarize the images shown in the beginning off this chapter, one can consult this summary table.

Table 1- Part result Summary

Corner	Overshoot axis	Corner finising	Ax	Ay
1	+y	Bad	-low	-low
2	-x	Good	+low	-high
3	-y	Bad	+low	+low
4	+x	Excellent	- low	+ high

So, we will have two corners that feel the effects of the stiffness in X and two that feel the effects of the stiffness in Y. Note again that considering that the distances from the TCP to the motors responsible for controlling the movement it is expected that this effect will have more and less impact in certain corners, as verified by the difference in printing quality on the four corners.

As the X-stiffness is higher, the corners that will be most affected will be the first and third. Note that the quality of the fourth corner is much better than the others. That information can also be confirmed by the data recovered by the accelerometer graph below.

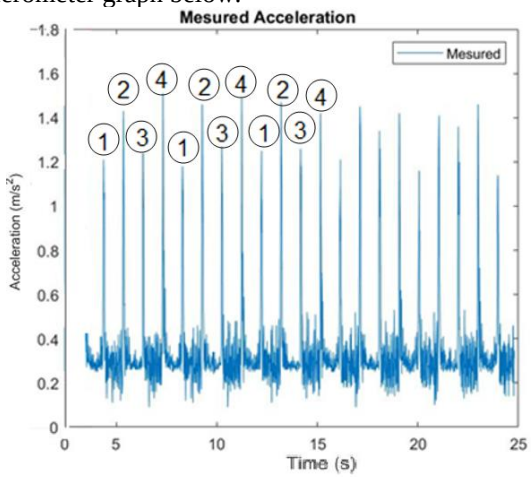

Figure 17-v50 measured acceleration with corner identification

Here, by analysis of the graph below, one can verify exactly what is obtained. When the robot goes through a more rigid corner it is expected that the acceleration felt in the TCP in the resonance direction is higher, since the robot is stiffer. When the acceleration is higher, position overshoot is lower, and repeatability is more easily guaranteed.

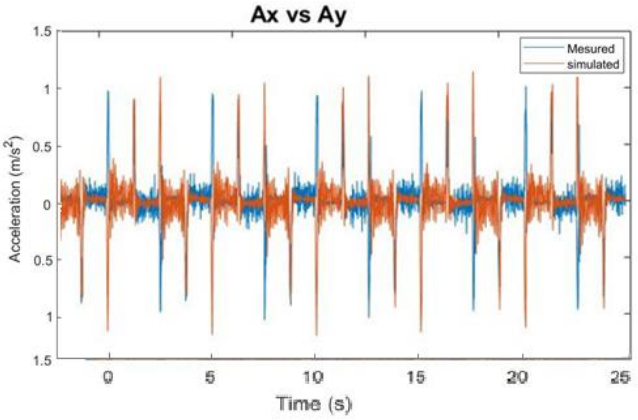

Figure 18-v50 Ax vs Ay

Obviously, the higher the speed, the more severe these effects are. At 60mm/s, these resonance effects start to make it impossible to print this part at an acceptable quality. Here again, and now with greater clarity, we can notice a clear difference between the four corners of the printed part.

D. Excessive speed test

As we know form the extruder tunning tests, it will no longer be possible to print parts at 70mm/s, due to the limitation of the maximum extrusion speed. Still, we would like to see what effects are observed in an extrusion attempt.

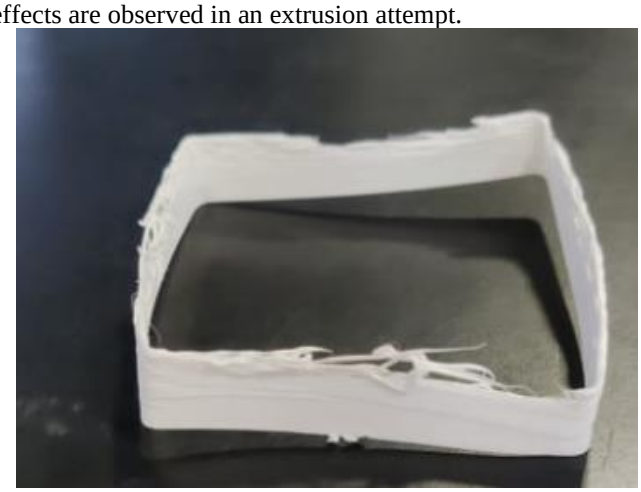

Figure 19- v70 results

We can see that here the effects of layer thickening and resonance in the corners is high. More importantly, as the extrusion speed cannot keep up with the forward speed of the robot, at the edge of the part, the filament gets successively thinner until it breaks at the top layers.

IV. Results

The objective of this work was based on the evaluation of this industrial robot as a positioner of a commercially available 3d printer head.

Thus, through the previous chapter we were able to understand the effects that different speeds can have on the quality of the surfaces and corners of a workpiece.

As we have seen, at speeds of 30 mm/s, the corners of the part remained stable, but under the compromise of a weaker surface finish.

At 40m mm/s we get a very interesting finishing results, with an almost perfect lateral surface finish and excellent corners.

On the other hand at 50 mm/s we have an excellent surface finish, under the compromise of a weaker corner finish.

With ease we understand that 60 mm/s is no longer an acceptable print quality, note that this test was done to exalt the maximum speed at which a print can produce stable results, under the conditions under which the test was done.

By today's 3D printing standards, the extrusion speeds achieved are considerably poor. Although it is important to point out that these prints were done at a constant extrusion speed and with a part that emphasizes these effects. Which means that, certainly, if it had been adjusted to the instantaneous speed of the robot, the results at these and higher speeds would be significantly improved. Still, this robot has a much higher stiffness than most commercially available printers, that can print at higher speeds, since low accelerations are used around corners, under a matching extrusion speed.

As for the material used, Siemens NX proved to be an excellent choice, allowing a high flexibility of operations that made this test specimen printing possible, and that will make possible future more complex projects related to the topics discussed. Also, the experimental material used proved to be capable of performing the intended tests. The only useful thing would have been the use of sensors capable of obtaining the real position of the robot's TCP, to be able to theoretically model this robot as a second-degree system.

Acknowledgements

This thesis was developed at Instituto Superior Técnico from University of Lisbon, Portugal, With the goal of understanding the capabilities of the ABB IRB 140 as an FDM 3D Printer positioner, successfully completed. This project would not be possible without my supervisors, Prof. Jorge Manuel Mateus Martins and Prof. João Carlos Prata dos Reis, who helped me technically and motivationally through the various stages of this thesis.

To Eng. João Eliseu from CADflow, whose tireless efforts helped me to solve various simulation problems, mainly related with RAPID post-processing.

I would also like to thank:

To Eng. António Tomás also from CADflow, for his sympathy and willingness in helping me solving problems in Siemens NX.

To José Vitorino from ABB Portugal, who helped me troubleshooting several problems regarding the Robot implementation.

To Eng. Camilo Christo for his sympathy and availability in helping me solving the most diverse problems in the Robotics laboratory.

To my colleague André Simões for his motivation and knowledge contribution.

And finally, to my family, who've always helped me, being essential in all my Academic journey.

REFERENCES

[1] J. Fernandes, A. M. Deus, L. Reis, M. F. Vaz, and M. Leite, “Study of the influence of 3D printing parameters on the mechanical properties of PLA,” in *Proceedings of the International Conference on Progress in Additive Manufacturing*, 2018, vol. 2018-May. doi: 10.25341/D4988C.

[2] L. Wang, W. M. Gramlich, and D. J. Gardner, “Improving the impact strength of Poly(lactic acid) (PLA) in fused layer modeling (FLM),” *Polymer*, vol. 114, 2017, doi: 10.1016/j.polymer.2017.03.011.

[3] K. G. Jaya Christiyan, U. Chandrasekhar, and K. Venkateswarlu, “Flexural Properties of PLA Components Under Various Test Condition Manufactured by 3D Printer,” *Journal of The Institution of Engineers (India): Series C*, vol. 99, no. 3, 2018, doi: 10.1007/s40032-016-0344-8.

[4] Vasco Gama Caldas Sampaio, “Towards Interaction Control of an Industrial Robotic Manipulator,” Lisbon, 2017.

[5] A. Robotics, “Application manual - Continuous Application Platform,” 2004.

[6] S. Vaidya, P. Ambad, and S. Bhosle, “Industry 4.0 - A Glimpse,” in *Procedia Manufacturing*, 2018, vol. 20. doi: 10.1016/j.promfg.2018.02.034.

[7] G. Erboz, “How to Define Industry 40: The Main Pillars of Industry 4.0,” *Managerial Trends in the Development of Enterprises in Globalization Era*, no. November 2017, 2017.

[8] L. Li, A. Haghighi, and Y. Yang, “A novel 6-axis hybrid additive-subtractive manufacturing process: Design and case studies,” *Journal of Manufacturing Processes*, vol. 33, 2018, doi: 10.1016/j.jmapro.2018.05.008.

[9] Kay Petermann, “SIX-AXIS ROBOT TURNS 3D PRINTING INTO AN ART FORM,” *Industrial Engneering news Europe*, Oct. 2017.

[10] Davide Sher, “+LAB Redefines the Composite Manufacturing Industry with the Atropos Kuka Robotic Arm,” *3D Printing Media Network*, Sep. 2016.

[11] Bruno Siciliano, Lorenzo Sciavicco, Luigi Villani, and Guiseppe Oriolo, *Advanced Textbooks in Control and Signal Processing*. London: Springer, 2009.

[12] Siemens, “Siemens Digital Industries Software,” Nov. 2021.

[13] Apple inc., “Getting Raw Accelerometer Events,” 2020.

[14] PROLIM, “ProLim,” 2021.

[15] Siemens, “Cavity Milling options, NX 1953 Series.” 2020.

[16] Siemens, “Planar additive operations dialog box, NX 1953 Series.” 2020.

[17] Siemens, “MOM events in multi-axis deposition postprocessors, NX 1953 Series.” 2020.